

**In: *The East African Great Lakes: Limnology, Paleolimnology and Biodiversity*,
Odada, E. O. and Olago, D. O (eds.), *Advances in Global Change Research*,
Kluwer Publishers, Dordrecht, 209–233, 2000.**

VENTILATION OF LAKE MALAWI / NYASA

M.K. VOLLMER¹, R.F. WEISS¹ and H.A. BOOTSMA²

¹*Scripps Institution of Oceanography, University of California at San Diego La Jolla, California,
92093–0244, USA*

²*Great Lakes WATER Institute, University of Wisconsin - Milwaukee,
Milwaukee, Wisconsin, 53204, USA*

ABSTRACT

A tracer study was conducted on Lake Malawi/Nyasa, one of the deepest and largest lakes in the world, in order to quantify the renewal rates of the deep water. For this purpose, concentrations of the anthropogenic trace gas chlorofluorocarbon-12 (CFC-12) were measured in water samples which were collected in glass ampoules and analyzed by a new gas chromatographic separation method. Based on measurements of stored duplicate samples, we conclude that the first-order degradation rate for CFC-12 in anoxic water of Lake Malawi/Nyasa lies in the range 0 to 0.012 yr⁻¹. The tracer measurements are used in a 3-box mixing model from which average exchange times between the hypolimnion and the metalimnion of 18.5 years and 15.9 years are calculated for the cases of no degradation and maximum degradation in anoxic water, respectively. These exchange times are 2.7 to 2.2 times higher than have been estimated previously based on tritium measurements in 1976 by Gonfiantini and coworkers. The exchange times between the metalimnion and the epilimnion are calculated to be 3.7 years and 3.4 years, again for no degradation and maximum degradation, respectively. These exchange times are comparable to those estimated previously. Volumetrically averaged apparent CFC-12 ages of 8.9 and 21.1 years were calculated for the metalimnion and the hypolimnion, respectively, under the assumption of no degradation. Latitudinal gradients in the CFC-12 and dissolved oxygen concentrations on isopycnal surfaces suggests that the deep water originates predominantly in the southern part of the lake.

1. INTRODUCTION

Lake Malawi/Nyasa, located in the East African Rift, is meromictic owing to a permanent but periodically weak stratification maintained by small gradients in temperature, salts, and dissolved uncharged species (Wüest *et al.*, 1996). As a consequence of this meromixis and the lake's internal biological cycle, the surface water is depleted in nutrients and biogenic material accumulates and decomposes in the partly anoxic deep water. As a result, the deep water is nutrient-rich, and total dissolved nutrient flux to the surface mixed layer is controlled to a large degree by vertical exchange within the lake. In order to study the cycling of these nutrients, the distribution of pollutants, and the lake's responses to external long-term perturbations, it is essential to know the deep-water renewal rates. In 1976, Gonfiantini *et al.* (1979) conducted a study of Lake Malawi/Nyasa using tritium produced by the atmospheric testing of thermonuclear weapons as a time-dependent tracer. Using a 3-box model, they calculated a 5-year average exchange time of the anoxic hypolimnion with respect to the metalimnion. The renewal time of the metalimnion with respect to the epilimnion was calculated to be 4 years.

The purpose of the current study is to give an independent estimate of deep-water renewal rates using measurements of the gaseous transient tracer CCl_2F_2 (chlorofluorocarbon-12 or CFC-12). Anthropogenically produced CFC-12 has been increasing in the atmosphere since its production began in the 1930s. This trace gas dissolves into the lake's surface water from the atmosphere, labeling the water with a time-dependent concentration signal as it is mixed into the interior of the lake. CFC-12 along with other chlorofluorocarbons (CFCs) have been used extensively in oceanographic studies (e.g. Gammon *et al.*, 1982; Weiss *et al.*, 1985; Pickart *et al.*, 1989; Doney and Bullister, 1992) to help understand the circulation and dynamics of the oceans. The successful application of CFC-12 as a limnological tracer in a study of Lake Baikal (Weiss *et al.*, 1991) has led to the application of this technique to Lake Malawi/Nyasa.

While CFC-12 is believed to be stable in oxygenated water, its stability in anoxic water is currently debated (Cook *et al.*, 1995; Oster *et al.*, 1996; Shapiro *et al.*, 1997; Plummer *et al.*, 1998). Laboratory experiments have shown CFC-12 degradation in anoxic soils and sediments (Lovley and Woodward, 1992; Oster *et al.*, 1996) but the applications of these results to an aqueous environment such as Lake Malawi/Nyasa have to be treated with caution as chemical and microbial conditions might differ significantly. Some of the studies in anoxic layers of groundwater (Cook *et al.*, 1995; Oster *et al.*, 1996), of a fjord (Shapiro *et al.*, 1997) and of lake waters (Aeschbach-Hertig *et al.*, 2001) have also suggested CFC-12 degradation under anoxia. However most of these studies are based on mixing models calibrated through inverse methods using other tracers, in particular tritium and helium-3. In these cases, temporal mixing variability together with different temporal evolutions of the atmospheric source functions for tritium and CFC-12 may lead to discrepancies in tracer loading to the water surface which, under the models' steady state assumptions, may show apparent CFC-12 degradation. In order to assess CFC-12 degradation in a manner

more applicable to the anoxic water of Lake Malawi/Nyasa, we have studied CFC-12 behavior in duplicate samples stored under anoxic conditions for more than 2 years.

2. METHODS

A hydrographic and geochemical survey was conducted on Lake Malawi/Nyasa (Figure 1) in September 1997 aboard R/V *Usipa*. CTD (conductivity-temperature-depth) data were collected by a Seabird SBE-19 profiler, fitted with an oxygen electrode, at 23 routinely visited stations along a north-south transect. At selected stations, the CTD casts were followed by a series of bottle casts, using 5-liter Hydro-Bios bottles, for the analysis of: nutrients, major ions, inorganic carbon species, and the isotopes $\delta^{13}\text{C}$ and $\Delta^{14}\text{C}$ of dissolved inorganic carbon; the transient tracers CFCs, helium-3 and tritium; and the gases N_2O and N_2/Ar . In addition to these selected stations, additional sampling for all the above-mentioned properties was performed at the location with the lake's maximum depth of 703 m (Station 940; $11^\circ 8.6'\text{S}$, $34^\circ 19.2'\text{E}$), northeast of Nkhata Bay. With the exception of helium-3 and tritium, all the measurements have been completed. Here we report the first interpretations of the hydrographic data and the CFC-12 results. CFC samples were collected at 3 stations (Figure 1), taking special precautions to avoid contamination from the sampling bottles and from ambient air (Bullister and Weiss, 1988). O-rings were vacuum-baked at 60°C for several days before installation at each end of the sampling bottles in order to lessen diffusive contamination into the sampled water. For the same purpose the internal rubber band in each bottle was replaced by an epoxy-coated stainless steel spring. Water sample aliquots were sealed into 100 ml custom-made Pyrex glass ampoules, following the technique developed by Busenberg and Plummer (1992) and modified by the Institute of Environmental Physics in Bremen (Klatt, 1997; Bulsiewicz *et al.*, 1998). For this purpose the glass ampoules were connected to the Hydro-Bios bottles via a stainless steel tubing fixture which allowed the flushing and filling of the ampoules. Immediately after filling, the ampoules were taken to the ship's laboratory for flame sealing with a propane-oxygen torch. A headspace was created in the ampoule's stem using ultra-high purity and CFC-free nitrogen gas. This headspace was needed to prevent cracking of the glass during the sealing process and to allow for potential thermal expansion of the water during transportation. The ampoules were kept dark and at ambient temperature while transported to the Scripps Institution of Oceanography for analysis.

Dissolved CFCs were analyzed by electron capture detection (ECD) gas chromatography in a modified purge-and-trap system originally designed by Bullister and Weiss (1988). The instrument was adapted for the ampoule technique, and the NaOH-impregnated absorbent Ascarite was used to remove traces of H_2S (Bullister and Lee, 1995) in order to avoid potential interference with the gases of interest. The water samples were kept in a water bath at 25.0°C before the glass

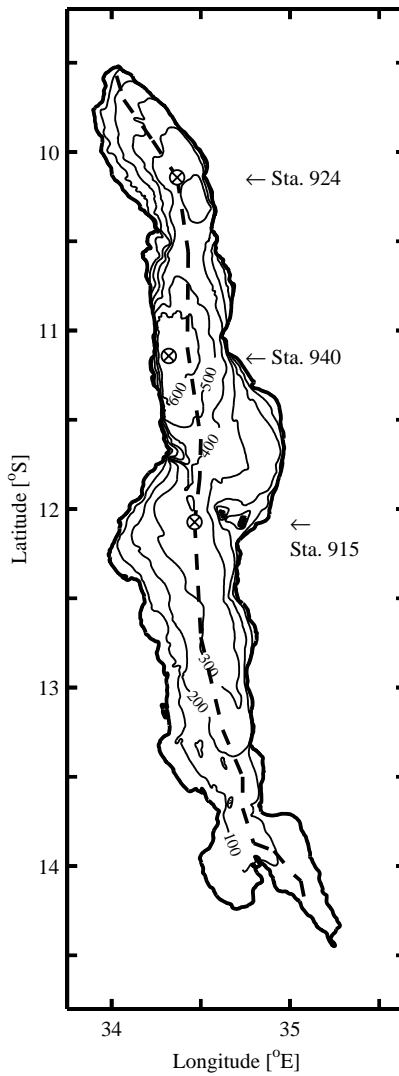


Figure 1. Bathymetric map for Lake Malawi/Nyasa including the section of routinely-visited stations (dashed line) and the locations of Stations 915, 924 and 940, where water samples for CFC-12 measurements were taken in September 1997. the 700 m isobath covers a small area in the vicinity of the Station 940 symbol and is not plotted for clarity.

ampoules were opened and aliquots were transferred to the purging chamber. Our first attempt to measure Lake Malawi/Nyasa samples using packed Porasil C columns (Bullister and Weiss, 1988) for chromatographic separation, was hindered by the presence of volatile hydrocarbons at elevated concentrations which interfered with the CFC peaks. The ECD responses to these hydrocarbons were negative and irregular when using P5 (5 % methane in argon) carrier gas, and these interferences affected mainly the quantification of the CFCs by peak area. Three samples were analyzed under these conditions and the results are included in this study, using peak height rather than peak area to determine their CFC concentrations. The chromatographic method was then altered to achieve a better separation of CFC-12 from the hydrocarbons. The sample gases were trapped in a short packed (Porasil C and Porapak T) column held at about -110°C (liquid nitrogen/methanol-ethanol slurry) and released after the trap was immersed into a hot water bath. Separation was achieved using a Porapak Q precolumn (40 cm) and main column (270 cm) at 150°C , followed by a molecular sieve 5A column (85 cm) at 160°C , all packed (80-100 mesh) in 1/8" OD stainless steel tubing. P5 carrier gas was used with a flow rate of 24 ml min^{-1} , and the precolumn was back-flushed 88 sec after injection. The gases were detected by a Shimadzu Mini-2 gas chromatograph with an ECD detector at 290°C . This revised chromatographic method did not allow for the measurement of CCl_3F (CFC-11) or $\text{CCl}_2\text{FCClF}_2$ (CFC-113), a compromise which was acceptable because these compounds are strongly degraded in anoxic waters (Bullister and Lee, 1995; Tanhua, 1997). Instead, the analytical method was optimized to measure CFC-12 and nitrous oxide (N_2O), with retention times of 350 sec and 480 sec, respectively. Corrections were made to account for the partitioning of these gases into the headspace of the ampoules. A first set of these samples was analyzed in February 1998. All other samples were stored dark and at room temperature until April 2000, when 33 of the remaining samples were analyzed under similar instrumental conditions in order to explore the possibility of CFC-12 degradation. Results for CFC-12 are reported on the SIO-1998 calibration scale (Prinn *et al.*, 2000). The analytical precisions (1σ , after applying a 3σ filter) for the CFC-12 standard gas were 0.3 % and 0.4 % for the Feb. 1998 and April 2000 analysis, respectively. The precisions for CFC-12 in the water samples reported as the mean of the relative standard deviations of duplicate samples during each analytical period were 2.3 % for Feb. 1998 ($n = 4$) and 0.4 % for April 2000 ($n = 3$).

3. RESULTS

The results for temperature, conductivity, dissolved oxygen and CFC-12 concentration profiles at the stations 915, 940 and 924 are listed in Table 1, and are plotted against depth together with the potential density anomaly in Figure 2. Depth was calculated from pressure using site-specific gravitational accelerations. In general we used the downcast hydrographic properties which we averaged in 5-m depth bins. These results are based on the calibration of the CTD sensors in 1996 and

are not corrected for possible sensor drift. We use distinct inflections in the oxygen and the CFC-12 concentration profiles at the deep Station 940 to distinguish three different layers in the lake, following a terminology suggested previously (Gonfiantini *et al.*, 1979). We thus designate the 105 m thick surface layer as the epilimnion, the middle layer as the metalimnion and the deep water below the oxic-anoxic boundary at approximately 220 m as the hypolimnion, realizing that these definitions do not match their more traditional meanings used to describe holomictic lakes.

Water temperature measured by the Seabird SBE-3 sensor is reported on the international temperature scale ITS-90. Potential temperature (Figure 2) was calculated from the CTD in-situ temperature according to Wüest *et al.* (1996) and includes the freshwater-specific adiabatic temperature gradient (Chen and Millero, 1986) but we integrated with respect to pressure instead of depth. The potential temperature decreases gradually throughout the epilimnion from about 25°C to 23.5°C indicating that the winter mixing has ended and spring stratification is well established. Throughout the metalimnion the potential temperature decreases downward with decreasing gradients. The lake reaches nearly isothermal conditions at about 22.7°C in the hypolimnion with a lowest value of 22.671°C found at 680 m at deep Station 940, which corresponds to an in-situ temperature of 22.787°C. In all our observed profiles temperature has an overall stabilizing effect on the water column, and in contrast to other authors (Wüest *et al.*, 1996; Patterson *et al.*, 1997) we found only inconclusive evidence of geothermal heating from inversions in the potential temperature for some of the profiles near the sediment-water interface. We also observed horizontal gradients in potential temperature along the transect of the routinely-visited stations (Figure 3a) resulting in isotherm outcropping in the southern part of the lake. Even though such a contour plot is a snapshot and internal seiching undoubtedly contributes to oscillations of the isotherms, there is support for this to be the prevalent condition in the lake, at least during the months of May to September (Hamblin *et al.*, 1999). The temperature profile for Station 924 differs significantly from the other stations. At this station a strong upwelling of epilimnetic and metalimnetic water is observed. Gradients in potential temperature and other CTD properties are large below a 20 m thick surface cap. Similar upwelling features have been observed in this region by Eccles (1974), who speculated that this may be associated with separate surface circulation cells driven by the local wind pattern, and by Patterson and Kachinjika (1995).

Although on a much finer scale than the upper waters, the abyss of Lake Malawi/Nyasa below a depth of about 300 m shows some horizontal temperature structure also (Figure 3a). Potential temperatures are higher at Stations 940 and 920 and decrease towards the north and south with typical gradients of a few hundredths of a degree per 100 km. The data for Station 940, which are not included in Figure 3, are similar to those at Station 920 for the lower part of the deep water and therefore support these observations. Such a feature could not have been observed during previous studies on the lake due to the lack of sufficient deep-water measurements, and it is therefore unclear whether it is permanent. Effects of internal waves or deep-water cooling from north and south may be possible explanations.

Table 1. Lake Malawi/Nyasa profiles for Stations 915, 940 and 924. In-situ temperature, in-situ conductivity and dissolved oxygen concentration from CTD downcast measurements. Potential temperature and reference conductivity κ_{20} are given in parentheses. The oxygen concentration measurements in the anoxic layer yielded slightly negative numbers and are not listed here. The CFC-12 concentrations from bottle samples are listed for those analyzed in February 1998 and in parentheses for those analyzed in April 2000. For both sets a correction is included for the loss of CFC-12 into the ampoules' headspaces. The CFC-12 results for the depths 10, 365 and 420 m at Station 924 were measured in Oct. and Nov. 1997 by a different chromatographic separation method (see text).

Depth [m]	<i>In-situ</i> (potential) Temperature [°C]	<i>In-situ</i> (reference) Conductivity [$\mu\text{S cm}^{-1}$]	Dissolved Oxygen [$\mu\text{mol kg}^{-1}$]	CFC-12 Concentration [pmol kg^{-1}]
Station 915 [12°18.5' S, 34°29.9' E] Sep. 14, 1997				
10	24.800 (24.798)	255.2 (230.0)	226.8	1.423
100	23.458 (23.441)	249.7 (231.4)	165.9	1.364 (1.343)
140	23.182 (23.158)	249.1 (232.0)	120.3	1.248 (1.259)
180	23.069 (23.038)	248.6 (232.1)	96.2	1.190 (1.191)
230	22.914 (22.875)	248.2 (232.4)	30.6	1.072 (1.037)
280	22.803 (22.756)	251.3 (235.7)	—	0.602
360	22.744 (22.684)	252.3 (236.8)	—	0.367 (0.354)
Station 940 [11°8.6' S, 34°19.2' E] Sep. 13, 1997				
10	25.124 (25.123)	257.3 (230.3)	225.9	1.422 (1.405)
50	24.251 (24.243)	252.8 (230.4)	187.9	1.404
105	23.563 (23.544)	250.6 (231.7)	167.6	1.369
120	23.365 (23.345)	250.0 (232.1)	121.3	1.273 (1.310)
140	23.171 (23.146)	249.4 (232.4)	90.7	1.198
170	23.068 (23.039)	249.1 (232.5)	70.9	1.145 (1.142)
190	23.011 (22.979)	248.8 (232.5)	43.2	1.067
200	22.987 (22.953)	248.7 (232.5)	30.2	1.041 (1.045)
215	22.972 (22.935)	248.6 (232.5)	23.0	0.998 (0.988)
230	22.922 (22.883)	248.7 (232.8)	—	0.908 (0.885)
245	22.882 (22.840)	249.8 (234.0)	—	0.821 (0.780)
300	22.817 (22.767)	251.1 (235.4)	—	0.573 (0.530)
360	22.780 (22.719)	251.9 (236.2)	—	0.474 (0.461)
420	22.774 (22.703)	252.1 (236.3)	—	0.425 (0.420)
480	22.770 (22.689)	252.3 (236.4)	—	0.401 (0.404)
530	22.772 (22.683)	252.5 (236.5)	—	0.389 (0.383)
570	22.775 (22.679)	252.6 (236.5)	—	0.382 (0.369)
610	22.779 (22.676)	252.7 (236.4)	—	0.378 (0.360)
640	22.782 (22.674)	252.7 (236.4)	—	0.373 (0.367)
670	22.786 (22.673)	252.8 (236.4)	—	0.360 (0.349)
685	22.786 (22.672)	252.8 (236.3)	—	0.359 (0.342)

	Station 924	[10°7.3' S, 34°18.4' E]		Sep. 10, 1997	
10	24.745 (24.744)	255.0	(230.2)	215.8	1.413
50	23.476 (23.467)	250.0	(231.6)	98.5	1.256 (1.264)
90	23.228 (23.213)	248.9	(231.8)	66.6	1.142 (1.154)
120	23.125 (23.105)	248.5	(231.8)	36.5	1.096 (1.083)
140	23.079 (23.055)	248.4	(231.9)	20.7	0.995 (0.917)
170	23.003 (22.975)	248.1	(232.0)	0.1	0.957 (0.933)
190	22.952 (22.920)	248.9	(233.0)	—	0.870 (0.854)
215	22.919 (22.883)	249.3	(233.4)	—	0.776
245	22.850 (22.809)	250.3	(234.6)	—	0.678 (0.667)
305	22.794 (22.743)	251.0	(235.4)	—	0.490 (0.495)
365	22.761 (22.701)	251.7	(236.2)	—	0.425
420	22.746 (22.676)	252.5	(236.8)	—	0.352
460	22.753 (22.676)	252.6	(236.8)	—	0.373

Unless geothermal warming has been drastically higher in this deep basin in recent years compared to the observations of Von Herzen and Vacquier (1967), this process seems an unlikely explanation for our observed horizontal temperature gradient as heat fluxes are generally low, and near Stations 940 and 920 were among the lowest found in the lake by these authors.

Based on in-situ electrical conductivity measured by the Seabird SBE-4 sensor, we have calculated the reference conductivity, κ_{20} , and the conductivity-based salinity according to the procedure described by Wüest *et al.* (1996). From the surface to maximum depth, κ_{20} and this salinity increased from about 230 to 236 $\mu\text{S cm}$ (Figure 2) and from about 0.210 to 0.215 g kg^{-1} , respectively. This salinity has a stabilizing effect on the density throughout the upper part of the water column, with the strongest gradient in the metalimnion and the upper hypolimnion. In the lower hypolimnion near Stations 920 and 940, κ_{20} and this salinity are practically uniform. Horizontal gradients of κ_{20} are small in general with the exception at Station 924 (Figure 3b). In the epilimnion a slight freshening of the water toward the north can be observed which could be an effect of higher rainfall and larger river inflow in the north, higher rates of evaporation in the south caused by strong southerlies and the resulting upwelling of water with higher conductivities.

We have used the silica concentration profiles (Bootsma and Hecky, 1999a) from this survey to calculate the non-ionic salinity (Wüest *et al.*, 1996). Assuming that the main silica component is silicic acid (Si(OH)_4), we find the non-ionic salinity to increase from 1.3 mg kg^{-1} in the epilimnion to 21.4 mg kg^{-1} at maximum depth which, in contrast to the results of Wüest *et al.* (1996), strengthens the stability of the entire water column.

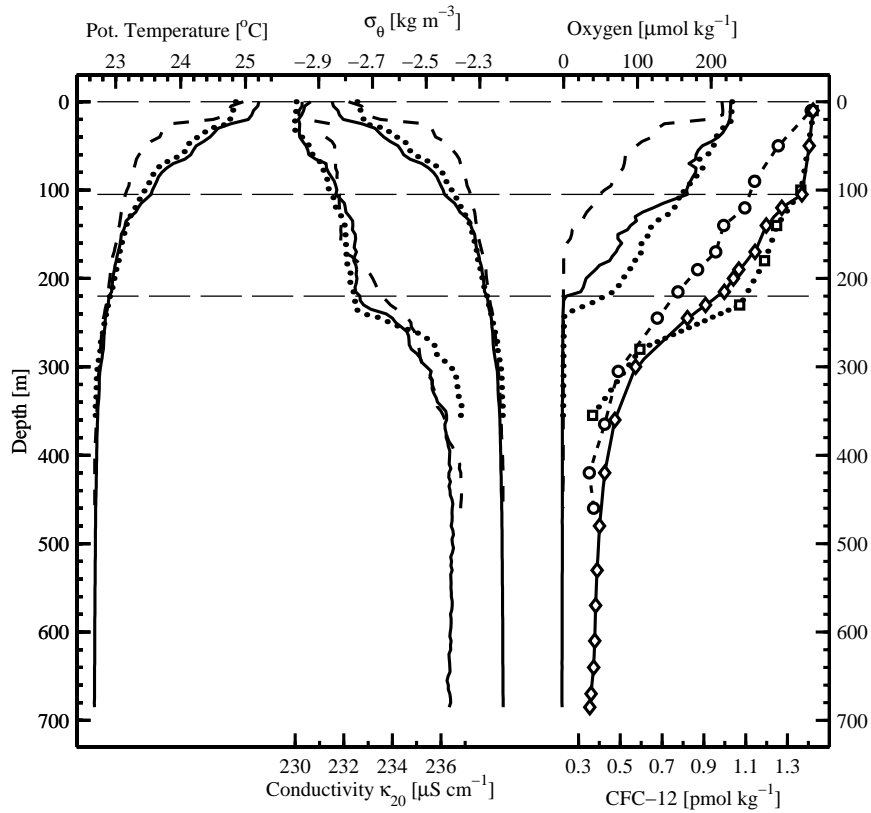


Figure 2. Vertical profiles at Stations 915 (dotted lines), 940 (solid lines) and 924 (dashed lines) of potential temperature (θ), reference conductivity (κ_{20}), potential density anomaly (σ_θ) and dissolved oxygen concentration from CTD measurements; and of CFC-12 concentration from water sample measurements. The CFC-12 results in this plot are based on the analytical measurements of February 1998. Horizontal dashed lines denote the lake's surface, and the boundaries between the epilimnion and metalimnion at 105 m and between the metalimnion and hypolimnion at 220 m.

Potential temperature and total salinity were used to calculate potential density (Figure 2) profiles (Wüest *et al.*, 1996; Chen and Millero, 1986). The potential density anomaly with respect to the lake surface (σ_θ) increases from about -2.75 kg m^{-3} at the surface to about -2.21 kg m^{-3} at greatest depth. The temperature gradient has a stronger effect on the density stratification than the salinity gradient.

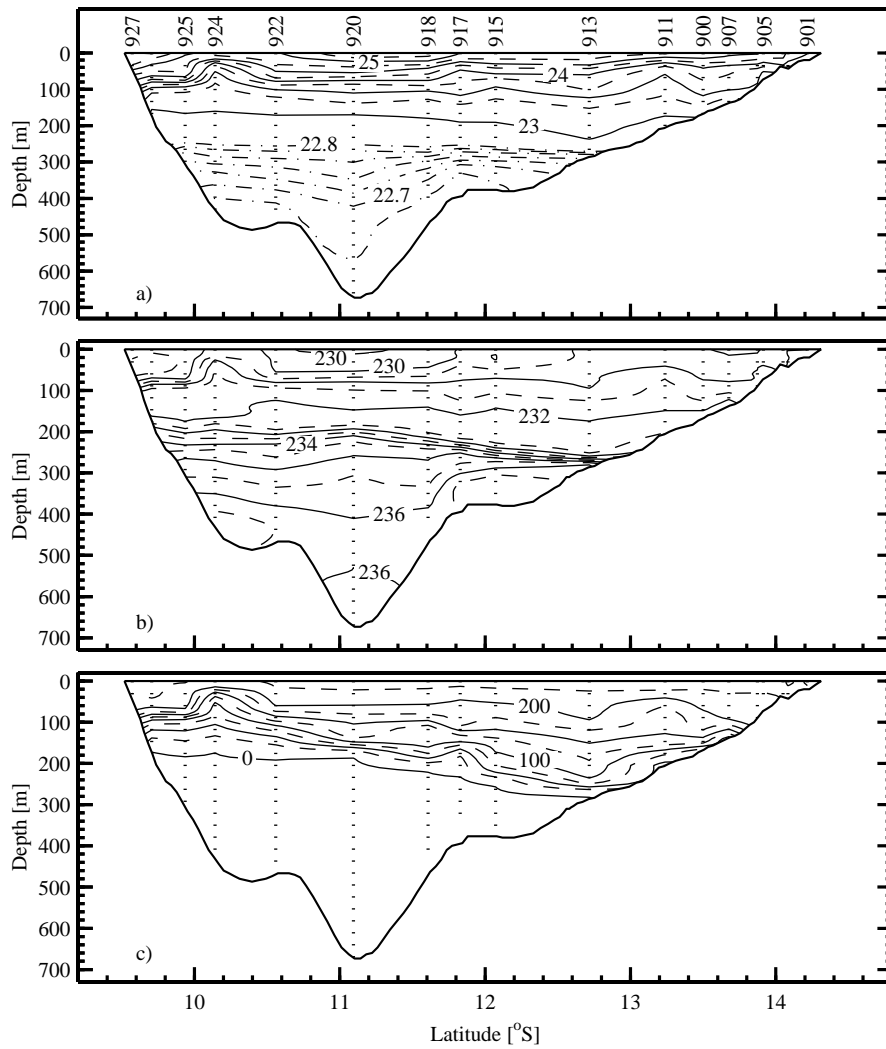


Figure 3. Objectively-mapped vertical contour section for CTD properties plotted against latitude south for the Sept. 1997 study on Lake Malawi/Nyasa, including stations along the routinely-visited north-south transect (see Figure 1). Deep Station 940 and stations in the southwest arm are excluded. Vertical dotted lines denote CTD depths at the latitudes of the stations occupied along this cruise track where as selected stations are labeled on the top. a) Potential temperature ($^{\circ}\text{C}$). Note the 0.25°C isotherm spacing above 23°C , and the 0.02°C spacing below 22.8°C . b) Reference conductivity κ_{20} ($\mu\text{S cm}^{-1}$). The dashed lines at greatest depth near Stations 915 and 924 indicate a conductivity of $236.5 \mu\text{S cm}^{-1}$. c) Dissolved oxygen ($\mu\text{mol kg}^{-1}$).

Between the epilimnetic-metalimnetic boundary and the maximum depth at deep Station 940, temperature, conductivity-based salinity and silica-based salinity contribute to the potential density increase by 95 %, 2 % and 3 %, respectively. The effect of the salinities on the density stratification is insignificant in the epilimnion and largest below the oxic-anoxic boundary where the two salinities contribute equally to the calculated density ratio (Wüest *et al.*, 1996) of about -0.15. Below a depth of about 400 m at Station 940, the conductivity-based density ratio fluctuates around a mean of essentially 0 and the mean silica-based density ratio is about -0.04. In this range the potential density is almost uniform but the stratification is stronger compared to the results of Wüest *et al.* (1996), as is indicated by a higher static stability, N^2 (Wüest *et al.*, 1996) which reaches a mean value of $6 \times 10^{-7} \text{ sec}^{-2}$ in the lowest observed 100 m of the lake.

The sound velocity profile (Chen and Millero, 1986) and a preliminary maximum depth for the water column at Station 940 were calculated for the depth of the CTD measurements using the acoustic travel time measured by the ship's echo sounder in this relatively large area of constant and maximum depth. An average sound velocity of 1497.4 m s^{-1} was calculated which includes an extrapolated sound velocity below the maximum depth of the CTD measurement. From this we calculate a maximum depth of 703 m taking into account the vertical displacement of 1.7 m of the echo sounder's transducer from the lake surface which was at the altitude of 473.3 m above sea level (Kingdon *et al.*, 1999) during the expedition. As for potential density, it is likely that non-ionic compounds and dissolved gases alter the sound velocity, thus altering the results for the maximum depth of the lake. Our calculated maximum depth is 3 m less than the maximum depth published by Hutchinson (1957) for an unreported lake stand at the time of these observations. In the rank of the world's deepest lakes, this newly-calculated Lake Malawi/Nyasa maximum depth still exceeds the maximum depth of Lake Issyk Kul (Hutchinson, 1957) by 1 m, or by much more if a recent depth measurement of about 660 m (T. Johnson, pers. comm.) for this brackish lake is used. Therefore Lake Malawi/Nyasa remains the world's 3rd deepest freshwater lake, or the 4th deepest lake if the brackish Caspian Sea is included.

The dissolved oxygen concentration was measured by the Seabird SBE-23B sensor. Dissolved oxygen concentration decreases with depth, with an anoxic layer below 170 m in the north and below 270 m in the south (Figure 3c). Dissolved oxygen is undersaturated throughout the water column. The volume-weighted dissolved oxygen concentration for the top 10 m of the water column is $230 \mu\text{mol kg}^{-1}$ which corresponds to a saturation of 94 % as calculated from the solubility function of Weiss (1970) at this layer's mean water temperature and salinity and for an annual mean atmospheric pressure (measured at Senga Bay) of 961 mbar (H. Bootsma, unpublished data).

The CFC-12 profiles for Stations 915 and 940 (Figure 2) show concentration decreases from the surface to the maximum depth, with distinct inflections at the interface between the top two layers. These transitions can also be seen in profiles of other properties, such as oxygen. At these 2 stations the epilimnetic CFC-12

concentrations are rather uniform at about 1.4 pmol kg^{-1} ($10^{-12} \text{ mol kg}^{-1}$), an indication that mixing during the preceding winter extended to a depth of about 100 m. At 10 m depth CFC-12 is saturated to 101 % with respect to a mean 1997 Southern Hemisphere atmospheric CFC-12 background concentration (data from Walker *et al.* (2000) converted to the SIO-1998 scale) of 531 ppt (dry air mole fraction in parts-per-trillion, or parts in 10^{12}), and a previously-mentioned reduced atmospheric pressure, as calculated from the solubility of CFC-12 (Warner and Weiss, 1985) at the local water temperatures and salinities. In the metalimnion, CFC-12 concentrations decrease to about 1 pmol kg^{-1} at the oxic-anoxic boundary, below which the CFC-12 concentrations decrease steeply to about 0.4 pmol kg^{-1} in the lower part of the hypolimnion. The CFC-12 concentration profile for Station 924 reflects the upwelling observed in the CTD properties. CFC-12 concentrations are lower than at the other two stations at similar depths in the lower epilimnion and in the metalimnion.

In order to estimate CFC-12 degradation in the anoxic water of Lake Malawi/Nyasa, we have measured duplicate samples more than 2 years after the first set of samples was analyzed. With a few exceptions from identical casts, the samples originated from duplicate casts with bottles at the same wire depths. The samples were stored dark and at a room temperature of about 23°C . Analyses were performed under similar conditions as for the first set, although some changes led to improvements in the overall precision of the measurements. For this second set of analyses, 14 out of 33 samples were from originally-oxygenated water in the lake, and the rest were from the anoxic zone. Some of the samples with low initial concentrations of dissolved oxygen may have become anoxic during storage. In particular we assume that this was the case for one sample (Station 924, 140 m) in which all the N_2O had disappeared during storage and this sample was therefore added to the group of anoxic samples. Interestingly this sample showed the largest decrease in CFC-12 concentration.

Most samples showed lower concentrations than their duplicates two years earlier (Figure 4). On average the initially-oxygenated samples yielded CFC-12 concentrations which were lower by $0.002 \text{ pmol kg}^{-1}$ (0.22 %), and the concentrations in the anoxic samples were lower by $0.018 \text{ pmol kg}^{-1}$ (3.1 %) than the previously analyzed samples. For the anoxic samples at Station 940, the absolute and relative differences between the two sample sets were found to be largest where the vertical concentration gradients are highest. This could be an artifact of slight changes in sampling depth for the two sets of samples taken from different casts during the expedition. For the oxygenated samples, no correlation was found between the observed concentration difference and the original oxygen or CFC-12 concentration. We assume no CFC-12 degradation in these samples, and we therefore conclude that the measured differences in the oxygenated samples are instrumental in nature. If we increase all the values in the second set by $0.002 \text{ pmol kg}^{-1}$ in order to remove this offset for the oxygenated samples, then the mean relative difference for the anoxic samples is -2.6 % which corresponds to a degradation rate of 0.012 yr^{-1} assuming this process to be first-order. We interpret this degradation rate with caution and as an upper limit. Analytical uncertainties may well have contributed to

the measured differences, as could a possible shift in bottle depth for the separate casts employed for these two sets of samples. In summary, from this study we can neither prove the existence nor the absence of CFC-12 degradation in Lake Malawi/Nyasa and we therefore pursue our calculations for both cases, no degradation and an upper limit of degradation as given above. The profiles in Figure 2 represent the first analytical set of samples listed in Table 1 and do not include a correction for potential degradation during the 5 month storage between dates of sampling and analysis.

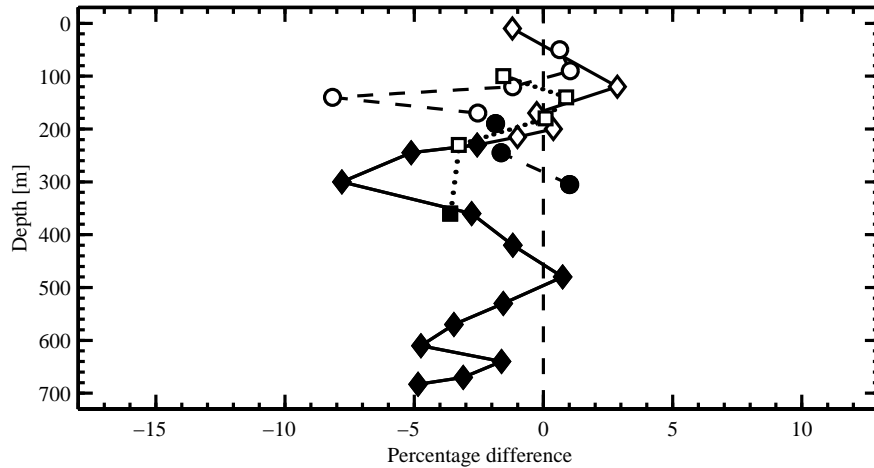


Figure 4. Results for the CFC-12 degradation study on Lake Malawi/Nyasa water samples stored in glass ampoules. Percentage differences are expressed as the April 2000 result minus the February 1998 result, divided by the mean of the two results and multiplied by 100. These are shown for Station 915 (squares), Station 924 (circles) and Station 940 (diamonds). Open and filled symbols represent initially-oxygenated and anoxic samples, respectively. A vertical dashed lines is drawn for zero concentration difference.

Our range of CFC-12 degradation rates from zero to 0.012 yr^{-1} for the anoxic water of Lake Malawi/Nyasa is less than most of those found in other anoxic waters. Our results are in agreement with the study of Shapiro *et al.* (1997) who have found “a maximum degradation rate of 0.01 to 0.03 yr^{-1} ” for an anoxic Norwegian fjord. Their results are based on a comparison between observed CFC-12 concentrations and those modeled using tritium and helium-3. Our results are an order of magnitude smaller compared to Aeschbach-Hertig *et al.* (2001) who have derived a CFC-12 degradation rate of 0.11 yr^{-1} for the anoxic layers of Lake Pavin using a similar

method to that of Shapiro *et al.* (1997). If we assumed zero-order CFC-12 degradation kinetics for our samples this would result in a maximum CFC-12 degradation of $0.011 \text{ pmol kg}^{-1} \text{ yr}^{-1}$, again a value which is significantly smaller than that deduced by Aeschbach-Hertig *et al.* (2001) of $0.07 \text{ pmol kg}^{-1} \text{ yr}^{-1}$ for Lake Pavin or than that found by Oster *et al.* (1996) of $0.08 \text{ pmol kg}^{-1} \text{ yr}^{-1}$ for groundwaters. Plummer *et al.* (1998) have found apparent stability of CFC-12 in ampoule samples filled with river water and stored for 2.5 yr under various conditions even though the samples were believed to have turned anoxic. However they also found complete loss of CFC-12 within 1 month of storage in glass ampoules in 2 samples of lake water. We believe that in those studies conducted so far there are significant inconsistencies in the determination of CFC-12 degradation, and that the observed differences may, at least in part, depend on the different chemical and biological conditions in different waters. For the case of Lake Malawi/Nyasa, we realize that only an improved degradation study using stored duplicate poisoned and unpoisoned samples from the same sampling bottles will lead to a clarification of this question.

4. MODEL CALCULATIONS

To calculate the exchange rates between the 3 layers we use a one-dimensional 3-box model similar to that used by Gonfiantini *et al.* (1979). The lake is divided vertically into the 3 layers separated at depths of 105 m and 220 m, and the exchange of water between adjacent layers is modeled. In contrast to Gonfiantini *et al.* (1979), who used a reconstructed epilimnetic tritium concentration as a forcing function, our model is forced by the atmospheric CFC-12 concentration evolution and by air-water gas exchange, and therefore the degree of CFC-12 saturation in the epilimnion is allowed to vary in our model. This replaces the approach in similar lake and most oceanic CFC studies, in which the epilimnetic CFC concentrations are assumed to be at a constant degree of saturation with respect to the increasing atmospheric CFC concentration. Such an assumption is justifiable for time periods when the rate of atmospheric increase remained essentially constant. However since the rate of increase of atmospheric CFC-12 has slowed considerably in recent years (Walker *et al.*, 2000) we have chosen to explicitly include the exchange of this tracer between the atmosphere and the epilimnion in our model calculations.

Accordingly, the exchange of water in the model is described by the following three coupled first-order differential equations,

$$\frac{dc_1}{dt} = \frac{V_2}{V_1} k_2 (c_2 - c_1) + \frac{A_s}{V_1} k_p (c_{sat} - c_1) \quad 1)$$

$$\frac{dc_2}{dt} = k_2 (c_1 - c_2) + k_3 \frac{V_3}{V_2} (c_3 - c_2) \quad 2)$$

$$\frac{dc_3}{dt} = k_3(c_2 - c_3) - j \cdot c_3 \quad 3)$$

and the water exchange fluxes between the epilimnion and the metalimnion, ϕ_2 , and between the metalimnion and the hypolimnion, ϕ_3 , are given by $\phi_2 = k_2 \times V_2$ and $\phi_3 = k_3 \times V_3$. The symbols c_i and V_i denote the CFC-12 concentrations and volumes of the epilimnion ($i = 1$), the metalimnion ($i = 2$) and the hypolimnion ($i = 3$), A_s is the lake's surface area, k_p is the air-water transfer velocity in units of m yr^{-1} , k_2 and k_3 are the epilimnetic-metalimnetic and metalimnetic-hypolimnetic exchange coefficients in units yr^{-1} , respectively, and j is the first-order degradation rate for CFC-12 in units of yr^{-1} . CFC-12 enters the epilimnion through air-water gas exchange following the atmospheric CFC-12 concentration history (Walker *et al.*, 2000), which is used here to calculate the saturation concentration, c_{sat} (Figure 5), for the salinity and pressure conditions described above, and an estimated epilimnetic winter temperature of 23.5°C as derived from a small inflection in the temperature profile at the lower boundary of this layer. We use only the tracer results of the deep Station 940, which we interpolated vertically by a cubic spline function to calculate the CFC-12 inventories in the 3 layers. We exclude Station 924 from this calculation because it reflects a region of strong upwelling which is not representative for this part of the lake (Figure 3). By excluding Station 924 we have also to exclude Station 915 to avoid an inventory bias due to an observed north-south gradient in CFC-12 as shown later. Station 940 appears to be a good average of the lake-wide CFC-12 distribution and due to this station's central position with respect to the north-south extensions, its water column is likely to be least effected by internal waves.

Using the hypsographic curve based on the unpublished bathymetric map of B. Halfman and T. Johnson (Large Lakes Observatory, University of Minnesota, Duluth), we calculate the layer volumes and the volumetrically averaged CFC-12 concentrations in the epilimnion, metalimnion and hypolimnion as: $2.76 \times 10^{12} \text{ m}^3$ and $1.40 \text{ pmol kg}^{-1}$, $2.31 \times 10^{12} \text{ m}^3$ and $1.16 \text{ pmol kg}^{-1}$, and $2.72 \times 10^{12} \text{ m}^3$ and $0.59 \text{ pmol kg}^{-1}$, respectively. These CFC-12 concentrations are based on the Feb. 1998 analytical results. For the calculations where $j = 0.012 \text{ yr}^{-1}$ these concentrations have been corrected for the 5-month storage of the samples.

CFC-12 concentrations for all 3 layers were calculated according to equations 1 to 3, for 0.1 yr time increments in the atmospheric concentration from 1931 to 1997 (Figure 5). Optimal k_i and k_p values were determined by least squares fitting to the observed mean CFC-12 concentrations. This resulted in exchange times (Table 2) between the layers of 3.7 yr for k_2^{-1} and 18.5 yr for k_3^{-1} assuming no CFC-12 degradation and 3.4 yr for k_2^{-1} and 15.9 yr for k_3^{-1} assuming $j = 0.012 \text{ yr}^{-1}$. In comparison, using their tritium profile, Gonfiantini *et al.* (1979) estimated k_2^{-1} and k_3^{-1} values of 4 yr and 5 yr, respectively.

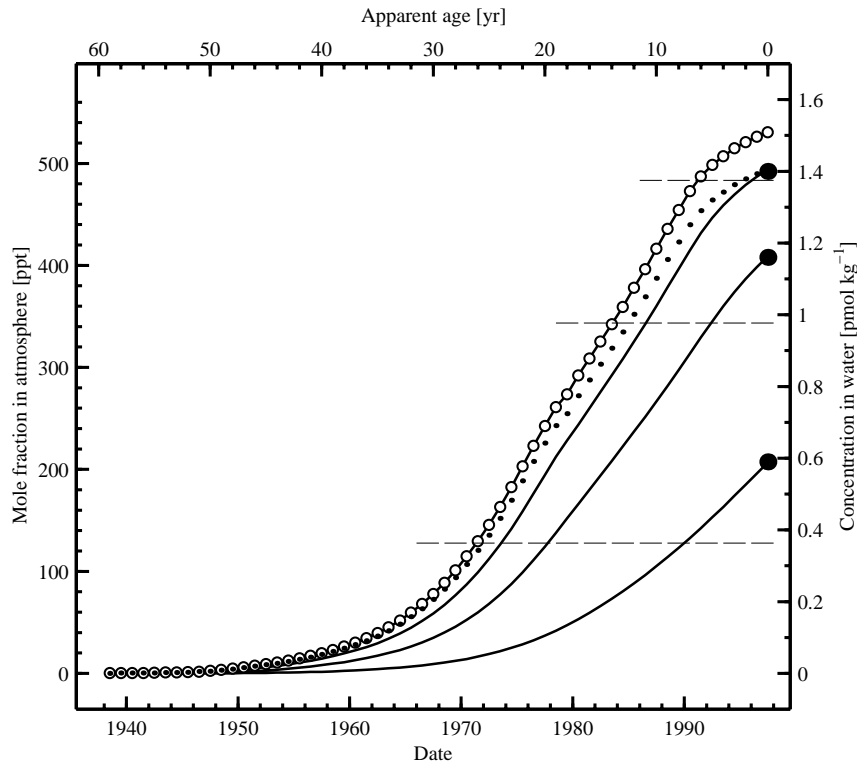


Figure 5. CFC-12 concentration reconstruction for the atmosphere and 3 box-layers in Lake Malawi/Nyasa. Atmospheric background concentrations vs. time (open circles) for CFC-12 in the Southern Hemisphere. Data are based on Walker *et al.* (2000) updated to the SIO-1998 calibration scale. The units are dry air mole fraction expressed as parts in 10^{12} (ppt), labeled on the left axis. The right axis gives CFC-12 concentrations in the water vs. time. The atmospheric record is equivalent to the epilimnion equilibrium concentration. The three solid lines ending in the volumetrically averaged layer concentrations (filled circles) for September 1997 are the results of our 3-box model. The dotted line was obtained by normalizing the atmospheric trend to a mean epilimnetic concentration of $1.40 \text{ pmol kg}^{-1}$ for September 1997 which corresponds to 93 % saturation at an estimated winter water temperature of 23.5°C . Dashed horizontal lines show the minimum CFC-12 concentration observed and the concentrations at the boundaries between the layers.

To make our results more directly comparable with those of Gonfiantini *et al.* (1979), the model calculations have also been performed for layers divided at 100 m and 250 m depths. The resulting volumetrically averaged CFC-12 concentrations were calculated as $1.41 \text{ pmol kg}^{-1}$, $1.13 \text{ pmol kg}^{-1}$, and $0.52 \text{ pmol kg}^{-1}$, for the

epilimnion, metalimnion and hypolimnion, respectively. Following this earlier study we also assumed equal layer volumes. The resulting exchange times (Table 2) between the layers are 4.7 yr for k_2^{-1} and 20.8 yr for k_3^{-1} assuming no degradation, and 4.5 yr for k_2^{-1} and 18.0 yr for k_3^{-1} assuming $j = 0.012 \text{ yr}^{-1}$. Again these results are of similar magnitude for the two upper layers and significantly higher for the two lower layers compared to the earlier tritium-based result.

5. DISCUSSION

The model-derived air-water transfer velocity k_p for CFC-12 when the layers are separated at 105 m and 220 m depths is calculated as 66 m yr^{-1} assuming no CFC-12 degradation and 69 m yr^{-1} including degradation. These results are based on the assumption of a constant year-round epilimnetic water temperature of 23.5°C and a mixed-layer thickness of 105 m, both of which are representative for the winter-time conditions. However gas exchange across the air-water interface is highly seasonal and effective only during part of the year. During spring and summer when the epilimnion is stratified, gas exchange is limited to a shallow surface mixed layer and, due to the warming during these periods, may result in supersaturation and subsequent outgassing of CFC-12. During this time the concentrations in the lower part of the epilimnion are expected to change little as mixing is greatly reduced. The important variables in the CFC-12 gas transfer are the onset of the seasonal cooling, the rate of the mixed layer deepening and the duration of a fully developed mixed layer before the next spring stratification begins. Our above assumption yields an overestimate of the term $c_{sat} - c_1$ (equation 1) which in turns results in an underestimate of the fitted mean annual transfer velocity k_p . If we assume gas exchange to be effective during a cooling period of about 6 months, an assumption based on multi-annual temperature observations (Patterson and Kachinjika, 1995), this would be equivalent to doubling our modeled k_p to a value of about 130 m yr^{-1} . We compare this value to the empirical transfer velocity k_p^* predicted by the air-sea gas exchange model of Wanninkhof (1992):

$$k_p^* = 87.6 \left[0.39 u^2 \left(\frac{Sc}{660} \right)^{-1/2} \right] \quad 4)$$

where u is the average winter wind speed, estimated as 2.5 m sec^{-1} from the data of Patterson and Kachinjika (1995), and Sc is the Schmidt number for CFC-12 in pure water (Zheng *et al.*, 1998), taken as 893 for the epilimnetic winter temperature of 23.5°C . This predicts a k_p^* value of 184 m yr^{-1} which is about one third larger than our estimated value. The modeled and predicted gas transfer rates agree surprisingly well considering that the Wanninkhof (1992) model is an empirical representation of open-ocean conditions with long wind fetch and breaking seawater

(rather than freshwater) waves, and also considering the large uncertainties in our choice of a 6-month period of effective gas exchange.

Table 2. Exchange times for the Lake Malawi/Nyasa 3-box model under various assumptions. Numbers in parentheses are for layer depth boundaries used by Gonfiantini *et al.* (1979). The first-order CFC-12 degradation rate for anoxic water is given by j .

		k_2^{-1} [yr]		k_3^{-1} [yr]	
This study	$j = 0 \text{ yr}^{-1}$	3.6	(4.7)	18.1	(20.3)
This study	$j = 0.012 \text{ yr}^{-1}$	3.4	(4.4)	15.6	(17.6)
Gonfiantini <i>et al.</i> (1979)			(4)		(5)

We have calculated the mean box model ages for the metalimnion and the hypolimnion. These ages are defined as the time elapsed since the water has last resided in the epilimnion and had therefore been in contact with the atmosphere. With this definition, the water age in the epilimnion is 0, and the mean box model ages of the water in the two subsurface boxes, τ_2 and τ_3 , are related to the exchange times by the relationships:

$$\tau_2 = \left(1 + \frac{V_3}{V_2}\right) \frac{1}{k_2} \quad 5)$$

and,

$$\tau_3 = \tau_2 + \frac{1}{k_3} \quad 6)$$

resulting in mean box model ages (Figure 6) of $\tau_2 = 8.0 \text{ yr}$ and $\tau_3 = 26.6 \text{ yr}$ in the case of no CFC-12 degradation and $\tau_2 = 7.5 \text{ yr}$ and $\tau_3 = 23.4 \text{ yr}$ for $j = 0.012 \text{ yr}$.

We have also calculated the CFC-12 apparent ages for the individual water samples collected at the deep Station 940. The apparent age of a water parcel approximates the time elapsed since it last resided in the epilimnion and hence was in contact with the atmosphere through gas exchange. We explicitly define the apparent age as the sampling date minus the date at which the epilimnion had the same CFC-12 concentration as is measured in the sample. We have used the local water temperatures and salinities and the time-dependent epilimnetic CFC-12 saturation derived from our modeled epilimnetic CFC-12 concentration to calculate dates at which the epilimnetic CFC-12 concentration was equal to the measured concentration in a sample. In Figure 6 the Station 940 CFC-12 apparent age profile is shown along with the box model ages for our CFC-12 based calculations. The volumetrically averaged CFC-12 apparent ages of the metalimnion and the hypolimnion are 8.9 yr and 21.1 yr, respectively.

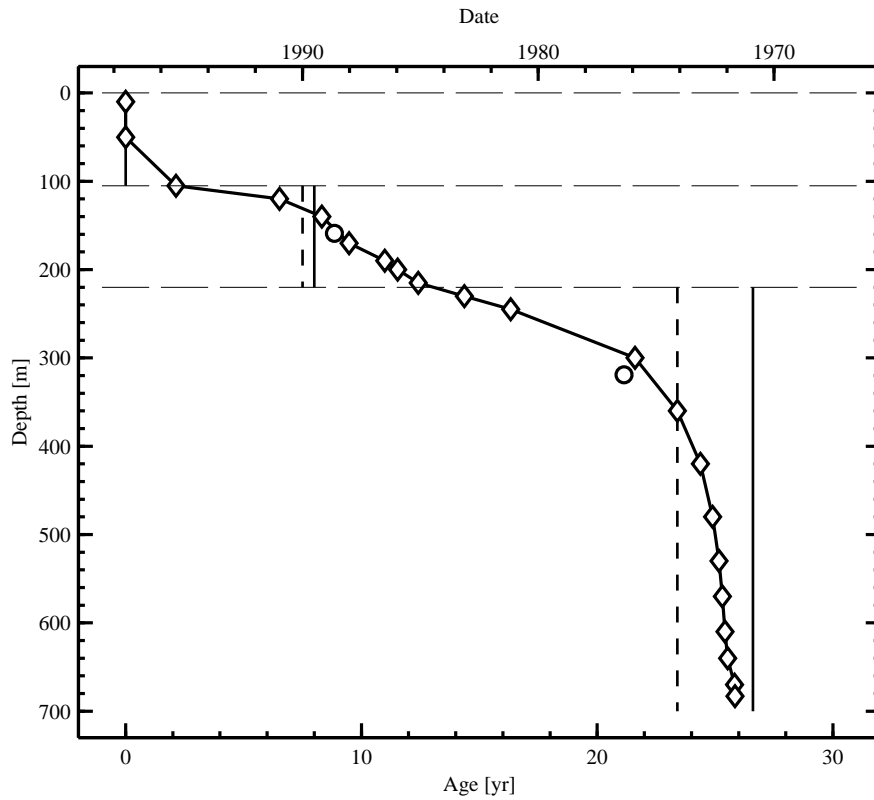


Figure 6. Age distribution for Lake Malawi/Nyasa water based on the CFC-12 concentration profile at Station 940. The CFC-12 apparent ages of the water samples (diamonds) and the box model ages for the case of no CFC-12 degradation (vertical solid lines) and a degradation rate of 0.012 yr^{-1} (vertical dashed lines) are shown vs. depth. The volumetrically averaged apparent ages (circles) for the hypolimnion and metalimnion are shown at the vertical volumetric midpoints of these layers. Horizontal dashed lines denote the lake's surface and the boundaries between epilimnion and metalimnion at 105 m and between metalimnion and hypolimnion at 220 m.

The apparent age of a water sample may differ from its mixing age because there is subsurface mixing in Lake Malawi/Nyasa. Here the mixing age is defined as the volume-weighted average of the individual ages of the components that comprise a mixture. In the special case where the CFC-12 atmospheric source function has been effectively linear over the range of ages of a mixture's components, the apparent age approximates the mixing age (Weiss *et al.*, 1991). Otherwise, mixing components

from an age range during which the CFC-12 atmospheric increase was accelerating with time (i.e. before the 1970s) will lead to an apparent age for the mixture which is less than the mixing age, while mixtures from an age range during which the atmospheric increase was decelerating with time (i.e. after the mid-1980s) will lead to an apparent age which is greater than the mixing age. The CFC-12 box model ages represent mean mixing ages, since mixing is included in the model. For the hypolimnion, the mean apparent age is lower than these box model ages and it is likely that the hypolimnetic apparent ages underestimate the mixing ages, since older (pre-1970s) individual water parcels undoubtedly contribute significantly to the mixtures in this part of the water column. For the metalimnion, where the mean apparent age is close to the box model ages, the contribution of young water might overestimate the mixing age and thus compensate for the age underestimation from older water which has upwelled into this layer. However it is impossible to quantify the mixing ages of the actual mixtures in the profile without a model which accurately represents the mixing history of the water column.

So far little attempt has been made to identify or quantify the physical processes involved with the ventilation of the deep water and this is not a goal of the present study. In the long-term, turbulent mixing across the pycnocline as simulated by the exchanges between the boxes in our model cannot be the only process of deep-water ventilation. To maintain the observed temperature gradient below the epilimnion, intrusions of cold water from the surface directly into the deeper layers must occur, thus compensating for heat diffusion from above and to a lesser extent for geothermal warming from the sediment. Such intrusions must result in an overall upwelling of the deep water, an hypothesis supported by the convex upward curvature of the vertical profiles of conservative properties such as potential temperature at depths below the influence of the seasonality of the upper water column.

It has long been recognized that ventilation of the Lake Malawi/Nyasa deep water may vary interannually. Beauchamp (1953) hypothesized that the deep water might warm and vertical temperature gradients decrease until an unusually cold 'cool season' triggers strong mixing which brings the lake to uniform temperature. As an alternative scenario it is likely that during extreme winters sinking cold water, produced in localized areas, feeds the deep water but that the vertical temperature gradients throughout most of the lake persist. Using the mean of the observed temperatures in the lower two strata at Station 940, our box model calculations result in a yearly temperature increase of the hypolimnion of 0.025°C , which includes a small geothermal warming (Von Herzen and Vacquier, 1967) of about $0.0008^{\circ}\text{C yr}^{-1}$. At steady state this warming must be compensated by cold water intrusions. Nevertheless the modeled warming of the hypolimnion is of similar magnitude as the observed temperature increases in the Lake Malawi/Nyasa deep water over the past six decades (Vollmer *et al.*, in preparation), suggesting that the hypolimnetic heat budget may not have been at steady state during this period.

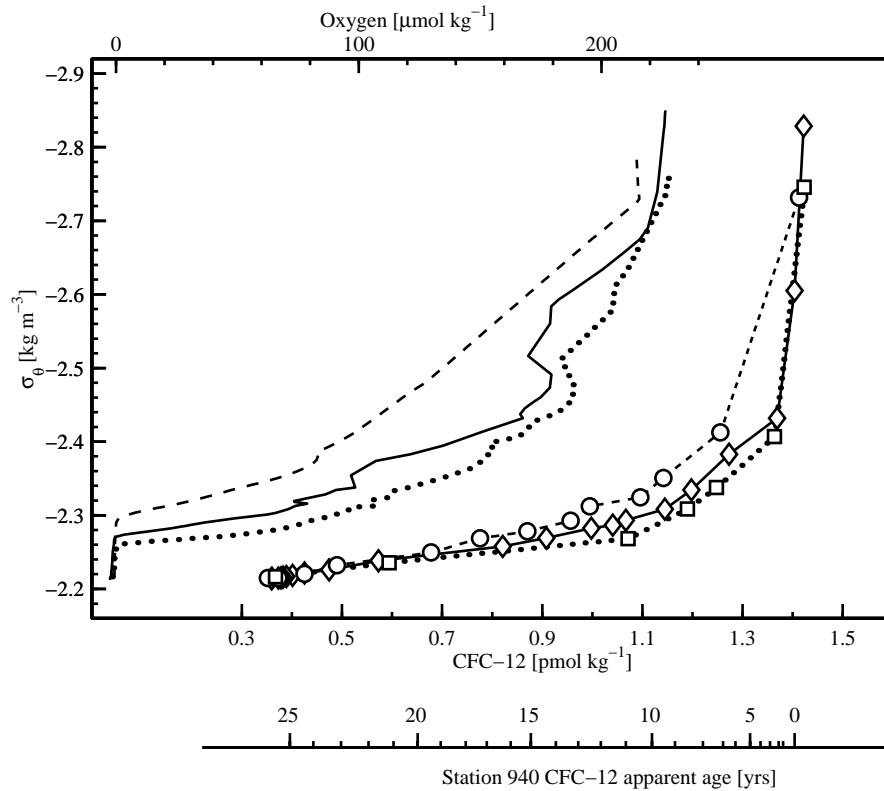


Figure 7. CFC-12 and dissolved oxygen concentrations plotted against potential density anomaly (σ_θ) for Stations 915 (dotted lines), 940 (solid lines) and 924 (dashed lines). CFC-12 concentrations show a northward decrease for the metalimnion and the upper hypolimnion hence a northward increase in apparent age and therefore suggest that deep-water ventilation is dominant in the south. The northward decrease in dissolved oxygen on equipotential density layers supports this finding.

The modeled warming of the metalimnion depends strongly on the mean temperature assumed for the epilimnion. For a scenario in which the epilimnion has a mean temperature lower limit of 23.5°C the metalimnion would warm by $0.08^\circ\text{C yr}^{-1}$ including geothermal warming of $0.002^\circ\text{C yr}^{-1}$. This or any warming based on calculations using higher epilimnetic temperatures, is too large to be maintained over decades and it is therefore likely that this layer receives cold water intrusions more frequently than the hypolimnion. Interannual variability in ventilation rates is also a possible explanation for the differences obtained between this and the earlier tracer study (Gonfiantini *et al.*, 1979). It may well be that deep-water ventilation was stronger in the 1960's when atmospheric tritium concentrations were largest while

ventilation has reduced during the last decade when atmospheric CFC-12 concentrations peaked.

Several mechanisms of cold water intrusion have been suggested, such as fluvial discharge, near-shore and open-water evaporative cooling during winter and turbidity currents (Halfman, 1993). The existence of such processes could be evidenced by a downward increase in CFC-12 concentrations near the lake floor which we do not find. However, without identifying specific processes, we find evidence that deep-water ventilation must primarily have occurred in the more southern parts of the lake in the past years. In Figure 7 we plot CFC-12 concentrations for our three stations against the potential density anomaly, rather than against depth, to eliminate effects of local vertical displacements of the water column by internal waves or upwelling. Significant differences in CFC-12 concentrations on isopycnals are observed in the metalimnion and upper hypolimnion with concentrations decreasing northward. The dissolved oxygen data also show northward concentration decreases and a corresponding shift of the oxic-anoxic boundary to lower density levels. These and the contoured oxygen data presented in Figure 3c support the CFC-12 based findings of older water in the north, although biases in the oxygen data can occur due to latitudinal changes in biological productivity and resulting changes in remineralization rates at depth.

The finding of a southern source of young deep water suggests that throughout the last decades deep plumes of fluvial discharge have not significantly contributed to the deep-water ventilation. Deep-water formation by river discharge is expected to be strongest in the northern part of the lake where the river inflows are larger and their water temperatures are lower than in the south (Kingdon *et al.*, 1999). This would lead to a northward decrease in deep-water ventilation age which is in contradiction to our findings from the CFC-12 observations.

6. CONCLUSION

Our 3-box model for CFC-12 in 1997 yields an exchange time between the hypolimnion and the metalimnion which is 2.2 to 2.7 times longer than that estimated by Gonfiantini *et al.* (1979) based on the tritium distribution they measured in 1976. These differences have significant effects in calculations of nutrient budgets and the residence times of compounds such as pollutants in the deep water. The reasons for this difference may be related to the incomplete representation of the actual mixing processes in this box model, including the transfer of these tracers from the atmosphere to the lake. These mixing rates must be treated with caution, since this 3-box model clearly oversimplifies the actual ventilation processes occurring in Lake Malawi/Nyasa. In fact, as noted earlier, this model cannot support steady-state temperature conditions because it does not allow for the direct intrusion of cold water from the surface into the hypolimnion. However it is likely that mixing conditions in Lake Malawi/Nyasa may experience variability on times scales of years to decades. A scenario of stagnant mixing conditions during the recent years when atmospheric CFC-12 concentrations were high or increased mixing during the early 1960's when

atmospheric tritium concentrations were high, is a possible explanation for the different results obtained from these two studies. It is hoped that the results of the analyses of our helium-3 and tritium samples, collected simultaneously with our CFC-12 samples, as well as an improved model representation, will lead to a more realistic characterization of deep-water ventilation rates. In addition, better characterization and quantification of mixing processes in Lake Malawi/Nyasa, as well as continuing tracer observations, are necessary in order to improve our understanding of deep-water renewal and its long-term variability.

ACKNOWLEDGMENTS

We thank the captain and the crew of R/V *Usipa* for their support of the expedition work, A. Krause for building the ampoule sampling devices, the group of W. Roether at the Institute of Environmental Physics in Bremen for their help with the ampoule technique, S. Walker for his help with the modeling calculations, and R. Hecky and the Canadian International Development Agency (CIDA) for their encouragement and financial support. This work has also been carried out under the auspices of the International Decade for the East African Lakes (IDEAL) program.

REFERENCES

- Aeschbach-Hertig W., Hofer M., Schmid M., Kipfer R., and Imboden D.M. (2001) The physical structure and dynamics of a deep, meromictic crater lake (Lac Pavin, France). *Hydrobio.*, in press.
- Beauchamp R.S.A. (1953) Hydrological data from Lake Nyasa. *J. Ecol.* **41**, 226-239.
- Bootsma H.A. and Hecky R.E. (1999a) Nutrient cycling in Lake Malawi/Nyasa, in Bootsma and Hecky (1999b), pp. 215-241.
- Bootsma H.A. and Hecky R.E. (eds.) (1999b) Water Quality Report; Lake Malawi Biodiversity Conservation Project. Southern African Development Community (SADC), Global Environmental Facility (GEF).
- Bullister J.L. and Lee B.S. (1995) Chlorofluorocarbon-11 removal in anoxic marine waters. *Geophys. Res. Lett.* **22**, 1893-1896.
- Bullister J.L. and Weiss R.F. (1988) Determination of CCl₃F and CCl₂F₂ in seawater and air. *Deep Sea Res.* **35**, 839-853.
- Bulsiewicz K., Rose H., Klatt O., Putzka A., and Roether W. (1998) A capillary-column chromatographic system for efficient chlorofluorocarbon measurement in ocean waters. *J. Geophys. Res.* **103**, 15,959-15,970.
- Busenberg E. and Plummer L.N. (1992) Use of chlorofluorocarbons (CCl₃F and CCl₂F₂) as hydrologic tracers and age-dating tools: the alluvium and terrace system of Central Oklahoma. *Water Resour. Res.* **28**, 2257-2283.
- Chen C.T.A. and Millero F.J. (1986) Precise thermodynamic properties for natural waters covering only the limnological range. *Limnol. Oceanogr.* **31**, 657-662.

- Cook P.G., Solomon D.K., Plummer L.N., Busenberg E., and Schiff S.L. (1995) Chlorofluorocarbons as tracers of groundwater transport processes in a shallow, silty sand aquifer. *Water Resour. Res.* **31**, 425–434.
- Doney S.C. and Bullister J.L. (1992) A chlorofluorocarbon section in the eastern North Atlantic. *Deep Sea Res.* **39**, 1857–1883.
- Eccles D.H. (1974) An outline of the physical limnology of Lake Malawi (Lake Nyasa). *Limnol. Oceanogr.* **19**, 730–742.
- Gammon R.H., Cline J., and Wisegarver D. (1982) Chlorofluoromethanes in the northeast Pacific Ocean: Measured vertical distributions and application as transient tracers of upper ocean mixing. *J. Geophys. Res.* **87**, 9441–9454.
- Gonfiantini R., Zuppi G.M., Eccles D.H., and Ferro W. (1979) Isotope investigation of Lake Malawi, in *Isotopes in Lake Studies*, International Atomic Energy Agency, Vienna. pp. 195–207.
- Halfman J.D. (1993) Water column characteristics from modern CTD data, Lake Malawi, Africa. *J. Great Lakes Res.* **19**, 512–520.
- Hamblin P.F., Bootsma H.A., and Hecky R.E. (1999) Modeling nutrient upwelling in Lake Malawi/Nyasa, in Bootsma and Hecky (1999b), pp. 123–141.
- Hutchinson G.E. (1957) *A Treatise on Limnology, Vol I. Geography, Physics and Chemistry*. Wiley, New York.
- Kingdon M.J., Bootsma H.A., Mwita J., Mwichande B., and Hecky R.E. (1999) River discharge and water quality, in Bootsma and Hecky (1999b), pp. 29–84.
- Klatt O. (1997) Entwicklungen am gaschromatographischen FCKW-Messsystem. Diploma thesis, University of Bremen.
- Lovley D.R. and Woodward J.C. (1992) Consumption of Freons CFC-11 and CFC-12 by anaerobic sediments and soils. *Environ. Sci. Technol.* **26**, 925–929.
- Oster H., Sonntag C., and Münnich K.O. (1996) Groundwater age dating with chlorofluorocarbons. *Water Resour. Res.* **32**, 2989–3001.
- Patterson G. and Kachinjika O. (1995) Limnology and phytoplankton ecology, in A. Menz (ed.), *The Fishery Potential and Productivity of the Pelagic Zone of Lake Malawi/Niassa*, Natural Resource Institute, Chatham, UK. pp. 1–67.
- Patterson G., Wooster M.J., and Sear C.B. (1997) Satellite-derived surface temperatures and the interpretation of the 3-dimensional structure of Lake Malawi, Africa: the presence of a profile-bound density current and the persistence of thermal stratification. *Verh. Internat. Verein. Limnol.* **26**, 252–255.
- Pickart R.S., Hogg N.G., and Smethie W.M. (1989) Determining the strength of the deep western boundary current using the chlorofluoromethane ratio. *J. Phys. Oceanogr.* **19**, 940–951.
- Plummer L.N., Busenberg E., Drenkard S., Schlosser P., Ekwurzel B., Weppernig R., McConnell J.B., and Michel R.L. (1998) Flow of river water into a karstic limestone aquifer —2. dating the young fraction in groundwater mixtures in the Upper Floridan aquifer near Valdosta, Georgia. *App. Geochem.* **13**, 1017–1043.
- Prinn R.G., Weiss R.F., Fraser P.J., Simmonds P.G., Cunnold D.M., Alyea F.N., O'Doherty S., Salameh P., Miller B.R., Huang J., Wang R.H.J., Hartley D.E., Harth C., Steele L.P., Sturrock G., Midgley P.M., and McCulloch A. (2000) A history of chemically and radiatively important gases in air deduced from ALE/GAGE/AGAGE. *J. Geophys. Res.* **105**, 17,751–17,792.

- Shapiro S.D., Schlosser P., Smethie Jr W.M., and Stute M. (1997) The use of ^3H and tritiogenic ^3He to determine CFC degradation and vertical mixing rates in Framvaren Fjord, Norway. *Mar. Chem.* **59**, 141–157.
- Tanhua T. (1997) Halogenated substances as marine tracers. PhD thesis, Göteborg University, Göteborg.
- Von Herzen R.P. and Vacquier V. (1967) Terrestrial heat flow in Lake Malawi, Africa. *J. Geophys. Res.* **72**, 4221–4226.
- Walker S.J., Weiss R.F., and Salameh P.K. (2000) Reconstructed histories of the annual mean atmospheric mole fractions for the halocarbons CFC-11, CFC-12, CFC-113, and carbon tetrachloride. *J. Geophys. Res.* **105**, 14,285–14,296.
- Wanninkhof R. (1992) Relationship between wind speed and gas exchange over the ocean. *J. Geophys. Res.* **97**, 7373–7382.
- Warner M.J. and Weiss R.F. (1985) Solubilities of chlorofluorocarbons 11 and 12 in water and seawater. *Deep Sea Res.* **32**, 1485–1497.
- Weiss R.F. (1970) The solubility of nitrogen, oxygen and argon in water and seawater. *Deep Sea Res.* **17**, 721–735.
- Weiss R.F., Bullister J.L., Gammon R.H., and Warner M.J. (1985) Atmospheric chlorofluoromethanes in the deep equatorial Atlantic. *Nature* **314**, 608–610.
- Weiss R.F., Carmack E.C., and Koropalov V.M. (1991) Deep-water renewal and biological production in Lake Baikal. *Nature* **349**, 665–669.
- Wüest A., Piepke G., and Halfman J.D. (1996) Combined effects of dissolved solids and temperature on the density stratification of Lake Malawi, in T.C. Johnson and E.O. Odada (eds.), *The Limnology, Climatology and Paleoclimatology of the East African Lakes*, Gordon and Breach, Amsterdam. pp. 183–202.
- Zheng M., DeBruyn W.J., and Saltzman E.S. (1998) Measurements of the diffusion coefficients of CFC-11 and CFC-12 in pure water and seawater. *J. Geophys. Res.* **103**, 1375–1379.